

Clustering in Hilbert simplex geometry

Frank Nielsen*

Ke Sun†

Abstract

Clustering categorical distributions in the probability simplex is a fundamental primitive often met in applications dealing with histograms or mixtures of multinomials. Traditionally, the differential-geometric structure of the probability simplex has been used either by (i) setting the Riemannian metric tensor to the Fisher information matrix of the categorical distributions, or (ii) defining the information-geometric structure induced by a smooth dissimilarity measure, called a divergence. In this paper, we introduce a novel computationally-friendly non-Riemannian framework for modeling the probability simplex: Hilbert simplex geometry. We discuss the pros and cons of those three statistical modelings, and compare them experimentally for clustering tasks.

Keywords: Fisher-Rao geometry, information geometry, Hilbert simplex geometry, center-based clustering.

1 Introduction

The multinomial distribution is an important representation in machine learning that is often met in applications [30, 16] as normalized histograms (with non-empty bins). A multinomial distribution (or categorical distribution) $p \in \Delta_d$ can be thought as a point lying in the probability simplex Δ_d (standard simplex) with coordinates $p = (\lambda_p^0, \dots, \lambda_p^d)$ such that $\lambda_p^i > 0$ and $\sum_{i=0}^d \lambda_p^i = 1$. The open probability simplex Δ_d sits in \mathbb{R}^{d+1} on the hyperplane $H_{\Delta_d} : \sum_{i=0}^d x_i = 1$. We consider the task of clustering a set $\Lambda = \{p_1, \dots, p_n\}$ of n categorical distributions [16] (multinomials) of Δ_d using center-based k -means++ or k -center clustering algorithms [5, 22] that rely on a dissimilarity measure (loosely called distance or divergence when smooth) between any two categorical distributions. In this work, we consider three distances with their underlying geometries for clustering: (1) Fisher-Rao distance ρ_{FHR} , (2) Kullback-Leibler divergence ρ_{IG} , and (3) Hilbert distance ρ_{HG} . The geometric structures are necessary in algorithms, for example, to define midpoint distributions. Figure 1 displays the k -center clustering results obtained with these three geometries. We shall now explain the Hilbert simplex geometry applied to the probability simplex, describe how to perform k -center clustering in Hilbert geometry, and report experimental results that demonstrate superiority of the Hilbert geometry when clustering multinomials.

1.1 Paper outline

The rest of this paper is organized as follows: Section 2 formally introduces the distance measures of Δ_d . Section 3 introduces how to efficiently compute the Hilbert distance. Section 4 presents algorithms for Hilbert minimax centers and Hilbert clustering. Section 5 performs an empirical study of clustering multinomial distributions, comparing Riemannian geometry, information geometry and Hilbert geometry. Section 6 concludes this work by summarizing the pros and cons of each geometry. Although some

*École Polytechnique, France and Sony Computer Science Laboratories Inc., Japan. E-mail: Frank.Nielsen@acm.org

†King Abdullah University of Science and Technology, Saudi Arabia.

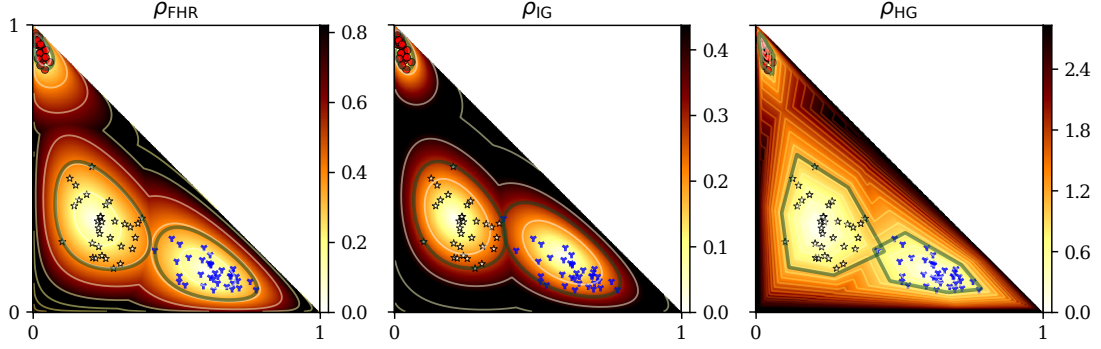


Figure 1: Clustering results on a toy dataset in the space of trinomials Δ_2 ($k = 3$ clusters). The color density maps indicate the distance from any point to its nearest cluster center.

contents require prior knowledge on geometric structures, we give clearly the algorithms so that general audience can still benefit from this work.

2 Three distances with their underlying geometries

2.1 Fisher-Hotelling-Rao geometry

The Rao distance of multinomials is [6]:

$$\rho_{\text{FHR}}(p, q) = 2 \arccos \left(\sum_{i=0}^d \sqrt{\lambda_p^i \lambda_q^i} \right).$$

It is a Riemannian metric length distance (satisfying the symmetric and triangular inequality axioms) obtained by setting the metric tensor g to the *Fisher information matrix* (FIM) I of the categorical distribution: $I(p) = [g_{ij}(p)]$ with

$$g_{ij}(p) = \frac{\delta_{ij}}{\lambda_p^i} + \frac{1}{\lambda_p^0}.$$

We term this geometry the Fisher-Hotelling-Rao (FHR) geometry [24, 51, 45, 46]. The metric tensor g allows to define an *inner product* on each tangent plane T_p of the probability simplex manifold: $\langle u, v \rangle_p = u^\top g(p)v$. When g is the identity matrix, we recover the Euclidean (Riemannian) geometry with the inner product being the scalar product: $\langle u, v \rangle = u^\top v$. The geodesics $\gamma(p, q; \alpha)$ are defined by the Levi-Civita metric connection [2, 14]. The FHR manifold can be embedded in the positive orthant of the Euclidean unit d -sphere of \mathbb{R}^{d+1} by using the *square root representation* $p \mapsto \sqrt{p}$, see [26]. Therefore the FHR manifold modeling of Δ_d has constant *positive curvature*.

2.2 Information geometry

A divergence D is a smooth C^3 differentiable dissimilarity measure [3] that allows to define a dual structure in Information Geometry [50, 14, 2] (IG). A f -divergence is defined for a strictly convex function f with $f(1) = 0$ by:

$$I_f(p : q) = \sum_{i=0}^d \lambda_p^i f \left(\frac{\lambda_q^i}{\lambda_p^i} \right).$$

It is a *separable* divergence since the d -variate divergence can be written as a sum of d univariate divergences: $I_f(p : q) = \sum_{i=0}^d I_f(\lambda_p^i : \lambda_q^i)$. The class of f -divergences plays an essential role in information theory since they are provably the *only* separable divergences that satisfy the *information monotonicity* property [2, 33]. That is, by coarse-graining the histograms we obtain lower-dimensional multinomials, say p' and q' , such that $0 \leq I_f(p' : q') \leq I_f(p : q)$, see [2]. The Kullback-Leibler (KL) divergence ρ_{IG} is a f -divergence obtained for $f(u) = -\log u$:

$$\rho_{\text{IG}}(p, q) = \sum_{i=0}^d \lambda_p^i \log \frac{\lambda_p^i}{\lambda_q^i}.$$

It is an asymmetric non-metric distance: $\rho_{\text{IG}}(p, q) \neq \rho_{\text{IG}}(q, p)$. In differential geometry, the structure of a manifold is defined by two components: (i) A *metric tensor* g that allows to define an inner product $\langle \cdot, \cdot \rangle_p$ at each tangent space (for measuring vector lengths and angles between vectors), and (ii) a *connection* ∇ that defines *parallel transport* $\prod_{p,q}^{\nabla}$, i.e., a way to move a vector from one tangent plane T_p to any other one T_q . For FHR geometry, the implicitly used connection is called the Levi-Civita connection that is induced by the metric g : $\nabla^{\text{LC}} = \nabla(g)$. It is a metric connection since it ensures that $\langle u, v \rangle_p = \langle \prod_{p,q}^{\nabla^{\text{LC}}} u, \prod_{p,q}^{\nabla^{\text{LC}}} v \rangle_q$. The underlying information-geometric structure of KL is characterized by a pair of dual connections [2] $\nabla = \nabla^{(-1)}$ (mixture connection) and $\nabla^* = \nabla^{(1)}$ (exponential connection) that induces two dual geodesics (technically, ± 1 -autoparallel curves [14]). Those connections are said *flat* as they define two dual affine coordinate systems θ and η on which the θ - and η -geodesics are straight line segments, respectively. For multinomials, the *expectation parameters* are: $\eta = (\lambda^1, \dots, \lambda^d)$ and they 1-to-1 correspond to the *natural parameters*: $\theta = \left(\log \frac{\lambda^1}{\lambda^0}, \dots, \log \frac{\lambda^d}{\lambda^0} \right)$. Thus in IG, we have two kinds of midpoint multinomials of p and q depending on whether we perform the (linear) interpolation on the θ - or the η -geodesics. Informally speaking, the dual connections $\nabla^{(\pm 1)}$ are said coupled to the FIM since we have $\frac{\nabla + \nabla^*}{2} = \nabla(g) = \nabla^{\text{LC}}$. Those dual connections are not metric connections but enjoy the following property: $\langle u, v \rangle_p = \langle \prod_{p,q}^{\nabla} u, \prod_{p,q}^{\nabla^*} v \rangle_q$, where $\prod = \prod^{\nabla}$ and $\prod^* = \prod^{\nabla^*}$ are the corresponding induced dual parallel transports. The geometry of f -divergences [3] is the α -geometry (for $\alpha = 3 + 2f'''(1)$) with the dual $\pm\alpha$ -connections, where $\nabla^{(\alpha)} = \frac{1+\alpha}{2}\nabla^* + \frac{1-\alpha}{2}\nabla$. The Levi-Civita metric connection is $\nabla^{\text{LC}} = \nabla^{(0)}$. More generally, it was shown how to build a dual information-geometric structure for *any* divergence [3]. For example, we can build a dual structure from the symmetric Cauchy-Schwarz divergence [25]:

$$\rho_{\text{CS}}(p, q) = -\log \frac{\langle \lambda_p, \lambda_q \rangle}{\sqrt{\langle \lambda_p, \lambda_p \rangle \langle \lambda_q, \lambda_q \rangle}}.$$

2.3 Hilbert simplex geometry

In Hilbert Geometry [23] (HG), we are given a *bounded convex domain* \mathcal{C} (here, $\mathcal{C} = \Delta_d$), and the distance between any two points M, M' of \mathcal{C} is defined as follows: Consider the two intersection points AA' of the line (MM') with \mathcal{C} , and order them on the line so that we have A, M, M', A' . Then the Hilbert metric distance [13] is defined by:

$$\rho_{\text{HG}}(M, M') = \begin{cases} \left| \log \frac{|A'M||AM'|}{|A'M'||AA'|} \right|, & M \neq M', \\ 0 & M = M'. \end{cases} \quad (1)$$

It is also called the Hilbert cross-ratio metric distance [17, 31]. Notice that we take the absolute value of the logarithm since the Hilbert distance is a *signed distance* [48]. When \mathcal{C} is the unit ball, HG let us recover the Klein hyperbolic geometry [31]. When \mathcal{C} is a quadric bounded convex domain, we obtain

Table 1: Comparing the three geometric modelings of the probability simplex Δ_d .

	Riemannian Geometry	Information Ric. Geo.	Non-Ric. Hilbert Geo.
Structure	$(\Delta_d, g) = (M, g, \nabla^{\text{LC}} = \nabla(g))$ Levi-Civita $\nabla^{\text{LC}} = \nabla^{(0)}$	$(\Delta_d, g, \nabla^{(\alpha)}, \nabla^{(-\alpha)})$ dual connections $\nabla^{(\pm\alpha)}$ so that $\frac{\nabla^{(\alpha)} + \nabla^{(-\alpha)}}{2} = \nabla^{(0)}$	(Δ_d, ρ) connection of \mathbb{R}^d
Distance	Rao distance (metric)	α -divergence (non-metric) KL or reverse KL for $\alpha = \pm 1$	Hilbert distance (metric)
Calculation	invariant by reparameterization closed-form	information monotonicity closed-form	isometric to normed space easy (Alg. 1)
Geodesic	minimizes length	straight either in θ/η	straight
Smoothness	manifold	manifold	non-manifold
Curvature	positive	dually flat	negative feature

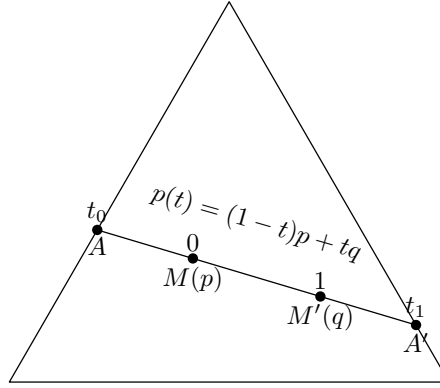


Figure 2: Computing the Hilbert distance for trinomials on the 2D probability simplex.

the Cayley-Klein hyperbolic geometry [12] which can be studied with the Riemannian structure and corresponding metric distance called the curved Mahalanobis distances [37, 36]. Cayley-Klein hyperbolic geometries have negative curvature.

In Hilbert geometry, the geodesics are *straight* Euclidean lines making it convenient for computation. Furthermore, the domain boundary $\partial\mathcal{C}$ need not to be smooth: One may also consider bounded polytopes [11]. This is particularly interesting for modeling Δ_d , the d -dimensional open standard simplex. We call this geometry: The *Hilbert simplex geometry*. In Fig. (2), we show that the Hilbert distance between two multinomials p (M) and q (M') can be computed by finding the two intersection points of the line $p(t) = (1-t)p + tq$ with $\partial\Delta_d$, denoted as $t_0 \leq 0$ and $t_1 \geq 1$. Then $\rho_{\text{HG}}(p, q) = \left| \log \frac{(1-t_0)t_1}{(-t_0)(t_1-1)} \right| = \left| \log(1 - \frac{1}{t_0}) - \log(1 - \frac{1}{t_1}) \right|$.

The shape of balls in polytope-domain HG are Euclidean polytopes [31], as depicted in Figure 3. Furthermore, the Euclidean shape of the balls do not change with the radius. Hilbert balls have hexagons shapes in 2D [42], rhombic dodecahedra shapes in 3D, and are polytopes [31] with $d(d+1)$ facets in dimension d . When the polytope domain is not a simplex, the combinatorial complexity of balls depends on the center location [42], see Figure 4. The HG of the probability simplex yields a non-Riemannian metric geometry because at infinitesimal radius value, the balls are polytopes and not ellipsoidal balls (corresponding to squared Mahalanobis distance balls used to visualize metric tensors [29]). The isometries in Hilbert polyhedral geometries are studied in [32].

Table 1 summarizes the characteristics of the three introduced geometries: FHR, IG, and HG.

3 Computing Hilbert distance in Δ_d

Let us first start by the simplest case: The 1D probability simplex Δ_1 , the space of Bernoulli distributions. Any Bernoulli distribution is represented by its activation probability $p \in \Delta_1$, and corresponds to a point in the interval $\Delta_1 = (0, 1)$.

3.1 1D probability simplex of Bernoulli distributions

By definition, the Hilbert distance has the closed form:

$$\rho_{\text{HG}}(p, q) = \left| \log \frac{q(1-p)}{p(1-q)} \right| = \left| \log \frac{p}{1-p} - \log \frac{q}{1-q} \right|.$$

Note that $\theta_p = \log \frac{p}{1-p}$ is the exponential family canonical parameters of the Bernoulli distribution.

For comparison, let us report the distance formula for KL and FHR: The Fisher information metric is given by: $g = \frac{1}{p} + \frac{1}{1-p} = \frac{1}{p(1-p)}$. The FHR distance is obtained by integration as:

$$\rho_{\text{FHR}}(p, q) = 2 \arccos \left(\sqrt{pq} + \sqrt{(1-p)(1-q)} \right).$$

The KL divergence of the ± 1 -geometry is:

$$\rho_{\text{IG}}(p, q) = p \log \frac{p}{q} + (1-p) \log \frac{1-p}{1-q}.$$

The KL divergence belongs to the family of α -divergences [2].

3.2 Arbitrary dimension case

Given $p, q \in \Delta_d$, we first need to compute the intersection of line (pq) with the border of the d -dimensional probability simplex to get the two intersection points p' and q' so that p', p, q, q' are ordered on (pq) . Once this is done, we simply apply the formula in Eq. 1 to get the Hilbert distance.

A d -dimensional simplex consists of $d+1$ vertices with their corresponding $(d-1)$ -dimensional facets. For the probability simplex Δ_d , let $e_i = (0, \dots, 1, 0, \dots, 0)$ denote the $d+1$ vertices of the

standard simplex embedded in the hyperplane $H_\Delta : \sum_{i=0}^{d-1} \lambda^i = 1$ in \mathbb{R}^{d+1} . Let $f_{\setminus j}$ denote the simplex facets that is the convex hull of all points e_i except e_j : $f_{\setminus j} = \text{hull}(e_1, \dots, e_{j-1}, e_{j+1}, e_{d+1})$. Let $H_{\setminus j}$ denote the hyperplane supporting this facet: The affine hull $f_{\setminus j} = \text{affine}(e_1, \dots, e_{j-1}, e_{j+1}, e_{d+1})$.

To compute the two intersection points of (pq) with Δ_d , a naive algorithm consists in computing the unique intersection point r of the line (pq) with each hyperplane $H_{\setminus j}$ ($j = 0, \dots, d$) and checking whether r belongs to $f_{\setminus j}$, or not.

A more efficient implementation given by Alg. (1) calculates the intersection points of the line $x(t) = (1-t)p + tq$ with all facets. These intersection points are represented using the coordinate t . For example, $x(0) = p$, $x(1) = q$, and any intersection point with $H_{\setminus j}$ must satisfy either $t \leq 0$ or $t \geq 1$. Then, the two intersection points are obtained by $t_0 = \max\{t : t \leq 0\}$ and $t_1 = \min\{t : t \geq 1\}$. This algorithm only requires $O(d)$ time.

Lemma 1 *The Hilbert distance in the probability simplex can be computed in optimal $\Theta(d)$ time.*

Once an arbitrary distance ρ is chosen, we can define a ball centered at c and of radius r as $B_\rho(c, r) = \{x : \rho(c, x) \leq r\}$. Figure 3 displays the hexagonal shapes of the Hilbert balls for various center locations in Δ_2 .

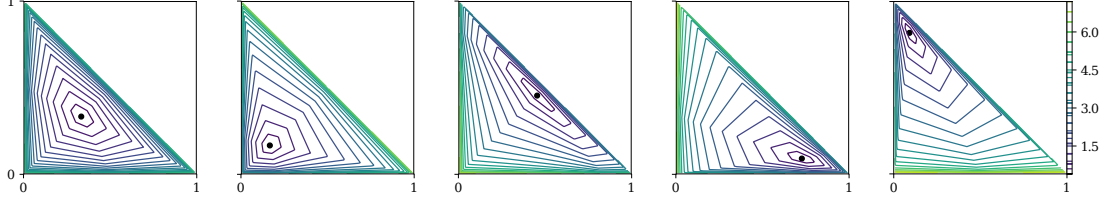


Figure 3: Balls in the Hilbert simplex geometry Δ_2 have polygonal Euclidean shapes of constant combinatorial complexity. At infinitesimal scale, the balls have hexagonal shapes thus showing that the Hilbert geometry is not Riemannian.

Algorithm 1: Computing the Hilbert distance

Data: Two points $p = (\lambda_p^0, \dots, \lambda_p^d), q = (\lambda_q^0, \dots, \lambda_q^d)$ in the d -dimensional simplex Δ_d
Result: Their Hilbert distance $\rho_{\text{HG}}(p, q)$

```

1 begin
2    $t_0 \leftarrow -\infty; t_1 \leftarrow +\infty;$ 
3   for  $i = 0 \dots d$  do
4     if  $\lambda_p^i \neq \lambda_q^i$  then
5        $t \leftarrow \lambda_p^i / (\lambda_p^i - \lambda_q^i);$ 
6       if  $t_0 < t \leq 0$  then
7          $t_0 \leftarrow t;$ 
8       else if  $1 \leq t < t_1$  then
9          $t_1 \leftarrow t;$ 
10  if  $t_0 = -\infty$  or  $t_1 = +\infty$  then
11    Output  $\rho_{\text{HG}}(p, q) = 0;$ 
12  else if  $t_0 = 0$  or  $t_1 = 1$  then
13    Output  $\rho_{\text{HG}}(p, q) = \infty;$ 
14  else
15    Output  $\rho_{\text{HG}}(p, q) = \left| \log\left(1 - \frac{1}{t_0}\right) - \log\left(1 - \frac{1}{t_1}\right) \right|;$ 

```

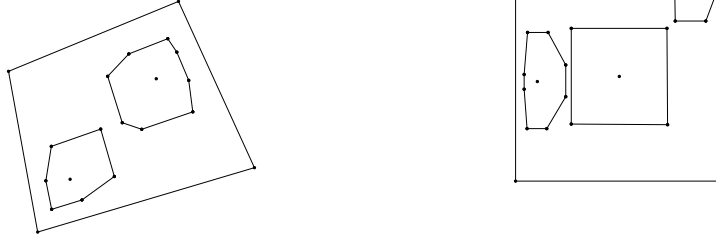


Figure 4: Hilbert Balls in quadrangle domains have combinatorial complexity depending on the center location.

Theorem 1 (Balls in a simplicial Hilbert geometry [31]) *A ball in a Hilbert simplex geometry has a Euclidean polytope shape with $d(d + 1)$ facets.*

Note that when the domain is not simplicial, the Hilbert balls can have varying combinatorial complexity depending on the center location. In 2D, the Hilbert ball polygonal shapes can range from s to $2s$ edges where s is the number of edges of the boundary Hilbert domain $\partial\mathcal{C}$.

Since a Riemannian geometry is locally defined by a metric tensor, at infinitesimal scales, Riemannian balls have Mahalanobis smooth ellipsoidal shapes: $B_\rho(c, r) = \{x : (x - c)^\top g(c)(x - c) \leq r^2\}$. This property allows one to visualize Riemannian metric tensors [29]. Thus we conclude that:

Lemma 2 ([31]) *Hilbert simplex geometry is a non-manifold metric length space.*

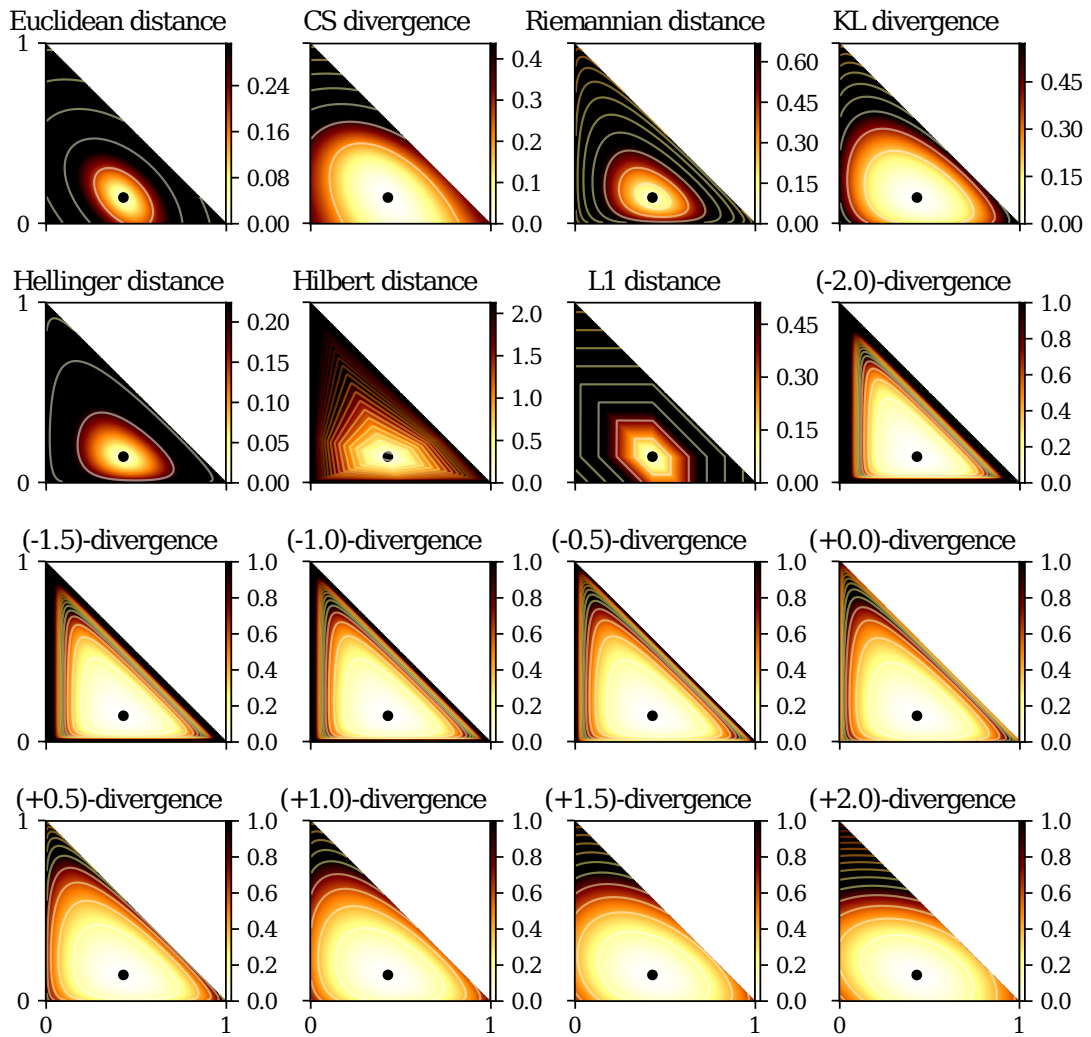
As a remark, let us notice that slicing a simplex with a hyperplane does not always produce a lower-dimensional simplex. For example, slicing a tetrahedron by a plane yields either a triangle or a quadrilateral. Thus the restriction of a d -dimensional ball B in a Hilbert simplex geometry Δ_d to a hyperplane H is a $(d - 1)$ -dimensional ball $B' = B \cap H$ of varying combinatorial complexity corresponding to a ball in the induced Hilbert sub-geometry with convex sub-domain $H \cap \Delta_d$.

3.3 Visualizing distance profiles

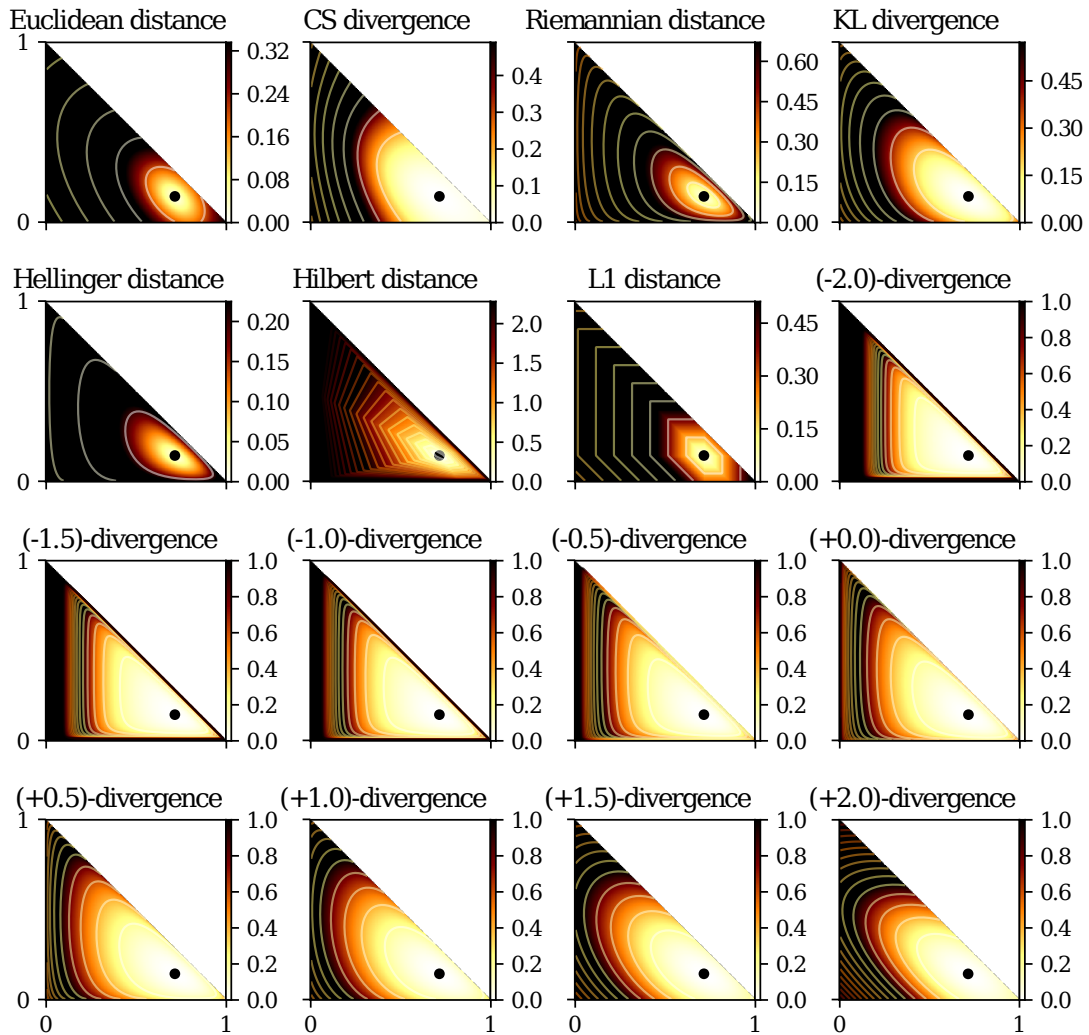
Figure 5 displays the distance profile from any point in the probability simplex to a fixed reference point (trinomial) for the following common distance measures [14]: Euclidean distance (metric), Cauchy-Schwarz (CS) divergence, Hellinger distance (metric), Fisher-Rao distance (metric), KL divergence and the Hilbert simplicial distance (metric). The Euclidean and Cauchy-Schwarz divergence are clipped to Δ_2 . The Cauchy-Schwarz distance is a projective distance $\rho_{CS}(\lambda p, \lambda' q) = \rho_{CS}(p, q)$ for any $\lambda, \lambda' > 0$, see [43].

4 Center-based clustering

We concentrate on comparing the efficiency of Hilbert simplex geometry for clustering multinomials. We shall compare the experimental results of k -means++ and k -center multinomial clustering for the three distances: Rao and Hilbert metric distances, and KL divergence. We describe how we implemented those clustering algorithms when dealing with a Hilbert distance.



(a) Reference point $(3/7, 3/7, 1/7)$



(b) Reference point $(1/7, 5/7, 1/7)$

Figure 5: A comparison of different distance measures on Δ_2 . The distance is measured from $\forall p \in \Delta_2$ to a fixed reference point (the black dot). Lighter color means shorter distance. Darker color means longer distance. The contours show equal distance curves with a precision step of 0.2.

4.1 k -Means++ clustering

The celebrated k -means clustering minimizes the sum of cluster variances, where each cluster has a center representative element. When dealing with $k = 1$ cluster, the center (also called centroid or cluster prototype) is the center of mass. For an arbitrary dissimilarity measure $D(\cdot : \cdot)$, the centroid c defined as the minimizer of

$$E_D(\Lambda, c) = \sum_{i=1}^n \frac{1}{n} D(\lambda_i : c),$$

may not be available in closed form. Nevertheless, using a generalization of the k -means initialization [5] (picking randomly seeds), one can bypass the centroid computation, and yet guarantee probabilistically a good clustering.

Let $C = \{c_1, \dots, c_k\}$ denote the set of k cluster centers. Then the generalized k -means energy to minimize is defined by:

$$E_D(\Lambda, C) = \sum_{i=1}^n \frac{1}{n} \min_{j \in \{1, \dots, k\}} D(\lambda_i : c_j).$$

By defining the distance $D(\lambda, C) = \min_{j \in \{1, \dots, k\}} D(\lambda : c_j)$ of a point to a set, we rewrite the objective function as follows: $E_D(\Lambda, C) = \sum_{i=1}^n \frac{1}{n} D(\lambda_i, C)$. Let $E_D^*(\Lambda, k) = \min_{C: |C|=k} E_D(\Lambda, C)$ denote the global minimum.

The k -means++ seeding proceeds for an arbitrary divergence D as follows: Pick uniformly at random at first seed c_1 , and iteratively choose the $(k - 1)$ remaining seeds according to the following probability distribution:

$$\Pr(c_i = x) = \frac{D^2(x, \{c_1, \dots, c_{i-1}\})}{\sum_{y \in \mathcal{X}} D^2(y, \{c_1, \dots, c_{i-1}\})}.$$

Since its inception (2007), this k -means++ seeding has been extensively studied [7]. We state the general theorem established in [40]:

Theorem 2 (Generalized k -means++ performance [40]) *Let κ_1 and κ_2 be two constants such that κ_1 defines the quasi-triangular inequality property:*

$$D(x : z) \leq \kappa(D(x : y) + D(y : z)), \forall x, y, z \in \Delta_d,$$

and κ_2 handles the symmetry inequality:

$$D(x : y) \leq \kappa_2 D(y : x), \forall x, y \in \Delta_d.$$

Then the generalized k -means++ seeding guarantee with high probability a configuration C of cluster centers such that:

$$E_D(\Lambda, C) \leq 2\kappa_1^2(1 + \kappa_2)(2 + \log k)E_D^*(\Lambda, k). \quad (2)$$

The ratio $\frac{E_D(\Lambda, C)}{E_D^*(\Lambda, k)}$ is called the competitive factor [5]. The seminal result of ordinary k -means++ yields a $8(2 + \log k)$ -competitive factor. Since divergences may be asymmetric, one can further consider mixed divergence $M(p : q : r) = \lambda D(p : q) + (1 - \lambda)D(q : r)$ for $\lambda \in [0, 1]$, and extend the k -means++ seeding procedure and analysis, see [41].

Note that squared metric distances are not metric because they do not satisfy the triangular inequality. For example, the squared Euclidean distance is not a metric but it satisfies the 2-quasi triangular inequality.

We state the following general performance theorem:

Theorem 3 (k -means++ in a normed space) *In any normed space $(\mathcal{X}, \|\cdot\|)$, the k -means++ seeding is $16(2 + \log k)$ -competitive.*

Proof: In a normed space, the parallelogram law holds:

$$2\|x\|^2 + 2\|y\|^2 = \|x + y\|^2 + \|x - y\|^2.$$

It follows that $\|x' - y'\|^2 \leq 2(\|x'\|^2 + \|y'\|^2)$ since $\|x' + y'\|^2 \geq 0$. Let $x' = x - z$ and $y' = y - z$ so that $x' - y' = x - y$ and, we get the 2-quasi triangular inequality.

$$\|x - y\|^2 \leq 2(\|x - z\|^2 + \|z - y\|^2).$$

Plugging $\kappa_1 = 2$ and $\kappa_2 = 1$ in Eq. 2, we get the $16(2 + \log k)$ -competitive factor. \square

The KL divergence can be interpreted as a separable Bregman divergence [1]. The Bregman k -means++ performance has been studied in [1, 34], and a competitive factor of $O(\frac{1}{\mu})$ is reported using the notion of Bregman μ -similarity.

In [20], it is proved that spherical k -means++ is $4(\log k + 2)$ -competitive, half of the ordinary k -means++. Therefore we get the lemma:

Lemma 3 (FHR k -means++ in Δ_d) *The squared Fisher-Hotelling-Rao k -means++ is $4(\log k + 2)$ -competitive for multinomials.*

Last, we need to report a bound for the squared Hilbert symmetric distance ($\kappa_2 = 1$). In [31] (Theorem 3.3), it was shown that Hilbert geometry of a bounded convex domain \mathcal{C} is isometric to a normed vector space iff \mathcal{C} is an open simplex: $(\Delta_d, \rho_{\text{HG}}) \simeq (\mathbb{R}^d, \|\cdot\|_H)$ where $\|x\|_H$ is the corresponding norm. Thus we get by applying Theorem 3:

Theorem 4 (k -means++ in Hilbert simplex geometry) *The k -means++ seeding in a Hilbert simplex geometry is $16(2 + \log k)$ -competitive.*

Note that for a given data set, we can compute κ_1 or κ_2 by inspecting triples and pairs of points, and get data-dependent competitive factor improving the bounds mentioned above.

4.2 k -Center clustering

Let \mathcal{X} be a finite point set. The cost function for a k -center clustering with centers \mathcal{C} ($|\mathcal{C}| = k$) is:

$$\max_{x \in \mathcal{X}} \min_{y \in \mathcal{C}} D(x : y).$$

The farthest first traversal heuristic of Gonzalez [22] has a guaranteed approximation factor of 2 for any metric distance (see Algorithm 2).

In order to use the k -center clustering algorithm described in Algorithm 4, we need to be able to compute a 1-center (or minimax center) for the Hilbert simplex geometry, that is the Minimum Enclosing Ball (MEB). In Riemannian geometry, the 1-center can be arbitrarily finely approximated by a simple geodesic bisection algorithm [9, 4] This algorithm can be extended to HG straightforwardly as detailed in Algorithm 3: The algorithm first picks up a point c_0 at random from \mathcal{X} for the initial center, computes the farthest point f_i (with respect to the distance ρ), and walk on the geodesic from c_0 to f_i by a certain amount to define c_1 , etc. For an arbitrary distance ρ , we define the operator $\#_\alpha^\rho$ as follows:

$$p\#_\alpha^\rho q = v = \gamma(p, q, \alpha), \quad \rho(p : v) = \alpha\rho(p : q),$$

where $\gamma(p, q, \alpha)$ is the geodesic passing through p and q , and parameterized by α ($0 \leq \alpha \leq 1$). When the equations of the geodesics are explicitly known, we can either get a closed form solution for $\#_\alpha^\rho$ or perform a bisection search on α to approximately compute α' such that $\rho(p : \gamma(p, q, \alpha')) = \alpha\rho(p : q)$. See [35] for an extension and analysis in hyperbolic geometry.

Algorithm 2: A 2-approximation of the k -center clustering for any metric distance ρ .

Data: A set \mathcal{X} , a number k of clusters and a metric ρ

Result: A 2-approximation of the k -center clustering

```

1 begin
2    $c_1 \leftarrow \text{RandomPointOf}(\mathcal{X});$ 
3    $\mathcal{C} \leftarrow \{c_1\};$ 
4   for  $i = 2 \dots k$  do
5      $c_i = \arg \max_{x \in \mathcal{X}} \rho(x, \mathcal{C});$ 
6      $\mathcal{C} \leftarrow \mathcal{C} \cup \{c_i\};$ 
7 Output  $\mathcal{C};$ 

```

Algorithm 3: Geodesic walk for approximating the Hilbert minimax center, generalizing [9]

Data: A set of points $p_1, \dots, p_n \in \Delta_d$. The maximum number T of iterations.

Result: $c = \arg \min_c \max_i \rho_{\text{HG}}(p_i, c)$

```

1 begin
2    $c_0 \leftarrow \text{RandomPointOf}(\{p_1, \dots, p_n\});$ 
3   for  $t = 1, \dots, T$  do
4      $p \leftarrow \arg \max_{p_i} \rho_{\text{HG}}(p_i, c_{t-1});$ 
5      $c_t \leftarrow c_{t-1} \#_{\frac{t}{t+1}} p;$ 
6   Output  $c_T;$ 

```

Furthermore, this iterative algorithm implies the proof of a core-set [10] (namely, the set of farthest points visited when iterating the geodesic walks) that is useful for clustering large data-sets [8].

Since Hilbert simplex geometry Δ_d is isometric to a normed space [21], there exists a Pythagorean theorem for the HG (i.e., $\|a + b\|^2 = \|a\|^2 + \|b\|^2$ for $a \perp b$), and the Euclidean proof of [9] that shows that Algorithm 4 generalizes:

Theorem 5 (MEB in a Hilbert simplex geometry) *The generalization of Badoiu and Clarkson iterative algorithm [9, 10] to approximate the 1-center in a Hilbert simplex geometry yields a $(1 + \epsilon)$ -approximation in $O(\frac{1}{\epsilon^2})$ iterations.*

See Fig (6) to get an intuitive idea on the convergence rate of Algorithm 3.

Thus by combining the k -center seeding of Gonzalez [22] with the iteration Lloyd-like batched iterations, we get an efficient k -center clustering algorithm for the FHR and Hilbert metric geometries. When dealing with the Kullback-Leibler divergence, we use the fact that KL is a Bregman divergence, and use the 1-center algorithm described in [44, 38] (approximation in any dimension) and [39] (exact but limited to small dimensions).

Since Hilbert simplex geometry is isomorphic to a normed vector space [31] with a polytope norm with $d(d + 1)$ facets, the Voronoi diagram in Hilbert geometry of Δ_d amounts to compute a Voronoi diagram with respect to a polytope norm [28, 47, 18].

5 Experiments

We generate a dataset consisting of a set of clusters in a high dimensional statistical simplex Δ_d . Each cluster is generated independently as follows. We first pick a random $c = (\lambda_c^0, \dots, \lambda_c^d)$ based on the

Hilbert distance with the true Hilbert center

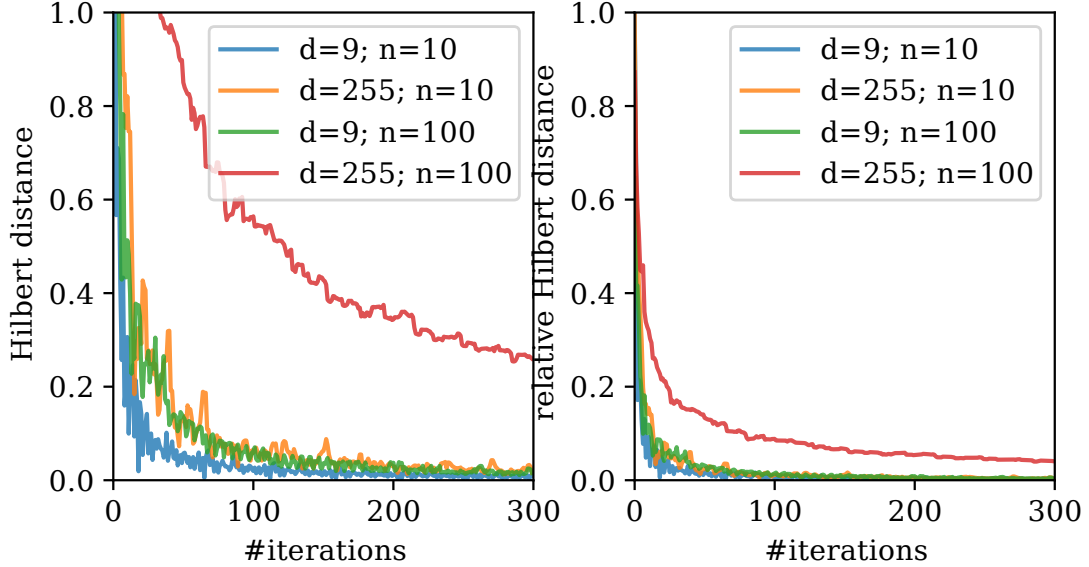


Figure 6: Convergence rate of Alg. (3) measured by the Hilbert distance between the current minimax center and the true center (left) or their Hilbert distance divided by the Hilbert radius of the dataset (right). The plot is based on 100 random points in Δ_9/Δ_{255} .

uniform distribution on Δ_d . Then we generate a random sample $p = (\lambda^0, \dots, \lambda^d)$ based on

$$\lambda^i = \frac{\exp(\log \lambda_c^i + \sigma \epsilon^i)}{\sum_{i=0}^d \exp(\log \lambda_c^i + \sigma \epsilon^i)}$$

where $\sigma > 0$ is a noise level parameter, and each ϵ^i follows independently a standard Gaussian distribution. Let $\sigma = 0$, we get $\lambda^i = \lambda_c^i$. Therefore p is randomly distributed around c . We repeat generating random samples for each cluster center, and make sure that different clusters have almost the same number of samples. Then we run k -center clustering in Alg. (4) based on the configurations $n \in \{50, 100\}$, $d \in \{9, 255\}$, $\sigma \in \{0.5, 0.9, 1.3\}$, $\rho \in \{\rho_{\text{FHR}}, \rho_{\text{IG}}, \rho_{\text{HG}}\}$. The number of clusters k is set to the true number of clusters to avoid model selection. For each configuration, we repeat the clustering experiment based on 300 different random datasets. The performance is measured by the cluttering accuracy, which is the percentage of clustering labels coinciding with the ground truth labels during the data generating process.

The results are shown in Table 2. The large variance of the accuracy is because that each experiment is performed on different datasets given by the same generator based on different random seeds. Generally, the performance deteriorates as we increase the number of clusters, increase the noise level or decrease the dimensionality, which have the same effect to reduce the gap among the clusters.

The key comparison is the three columns ρ_{FHR} , ρ_{HG} and ρ_{IG} , as they are based on exactly the same algorithm (k -center) with the only difference being the underlying geometry. We see clearly that the performance of the three compared geometries presents the order $\text{HG} > \text{FHR} > \text{IG}$. The performance of HG is superior to the other two geometries, especially when the noise level is large. Intuitively, the Hilbert balls are more compact and therefore can better capture the clustering structure (see Fig. (1)).

Algorithm 4: k -center clustering

Data: A set of points $p_1, \dots, p_n \in \Delta_d$. A distance measure ρ on Δ_d . The maximum number k of clusters. The maximum number T of iterations.

Result: A clustering scheme assigning each p_i a label $l_i \in \{1, \dots, k\}$

```
1 begin
2   Randomly pick  $k$  cluster centers  $c_1, \dots, c_k$  using the kmeans++ heuristic;
3   for  $t = 1, \dots, T$  do
4     for  $i = 1, \dots, n$  do
5        $l_i \leftarrow \arg \min_{l=1}^k \rho(p_i, c_l)$ ;
6     for  $l = 1, \dots, k$  do
7        $c_l \leftarrow \arg \min_c \max_{i:l_i=l} \rho(p_i, c)$ ;
8   Output  $\{l_i\}_{i=1}^n$ ;
```

The column ρ_{IG} (k -means) is the k -means clustering based on ρ_{IG} . It shows better performance than ρ_{IG} because k -means is more robust than k -center to noise. Ideally we should compare k -means based on FHR, IG and HG. However the centroid computation of FHR and HG are not developed yet. This is left to future work.

The column ρ_{EUC} represents k -center based on the Euclidean enclosing ball. It shows the worst scores because the intrinsic geometry of the probability simplex is far from being Euclidean.

6 Conclusion

We introduced the Hilbert metric distance and its underlying non-Riemannian geometry for modeling the space of multinomials of the open probability simplex, and compared experimentally this geometry with the traditional differential-geometric modelings (either FHR metric connection or dually coupled non-metric affine connection of information geometry [2]) for clustering tasks. The main feature of HG is that it is a metric non-manifold geometry where geodesics are straight (Euclidean) line segments. For simplex domains, the Hilbert balls have fixed combinatorial (Euclidean) polytope structures, and HG is known to be isometric to a normed space [21]. This latter isometry allows one to generalize easily the standard proofs of clustering (e.g., k -means or k -center). We demonstrated it for the k -means++ competitive performance analysis, and for the convergence of the 1-center heuristic [9] (smallest enclosing Hilbert ball allows one to implement efficiently the k -center clustering). Our experimental k -means++/ k -center comparisons of HG algorithms with the manifold modeling approach yield striking superior performance: This may be explained by the sharpness of Hilbert balls with respect to the FHR/IG ball profiles.

Chentsov [15] defined statistical invariance on a probability manifold under Markov morphisms, and proved that the Fisher Information Metric (FIM) is the unique Riemannian metric (up to rescaling) for multinomials. However, this does not rule out that other distances (with underlying geometric structures) may be used to model statistical manifolds (eg., Finsler statistical manifolds [49], or the total variation distance — the only metric f -divergence [27]). Defining statistical invariance related to geometry is the cornerstone problem of information geometry that can be tackled from many directions (see [19] and references therein for a short review). We hope to have fostered interest in considering the potential of Hilbert probability simplex geometry in artificial intelligence. One future direction is to consider the Hilbert metric for regularization and sparsity in machine learning (due to its equivalence with a polytope normed distance).

Our Python codes are freely available online for reproducible research:

<https://www.lix.polytechnique.fr/~nielsen/HSG/>

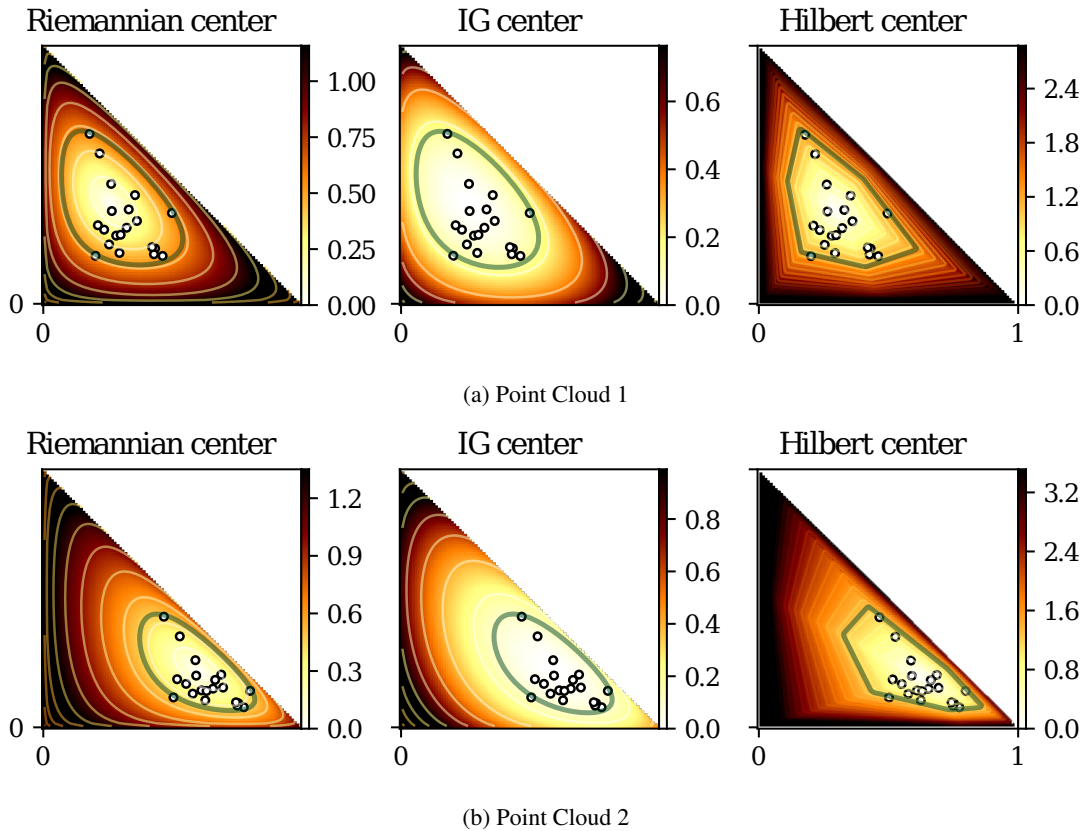


Figure 7: The Riemannian/IG/Hilbert (from left to right) minimax centers of two point clouds in Δ_2 based on Alg. (3). The color maps show the distance from $\forall p \in \Delta_2$ to the corresponding center.

References

- [1] Marcel R Ackermann and Johannes Blömer. Bregman clustering for separable instances. In *Scandinavian Workshop on Algorithm Theory*, pages 212–223. Springer, 2010.
- [2] Shun-ichi Amari. *Information Geometry and Its Applications*. Applied Mathematical Sciences. Springer Japan, 2016.
- [3] Shun-ichi Amari and Andrzej Cichocki. Information geometry of divergence functions. *Bulletin of the Polish Academy of Sciences: Technical Sciences*, 58(1):183–195, 2010.
- [4] Marc Arnaudon and Frank Nielsen. On approximating the Riemannian 1-center. *Computational Geometry*, 46(1):93–104, 2013.
- [5] David Arthur and Sergei Vassilvitskii. k -means++: The advantages of careful seeding. In *ACM-SIAM symposium on Discrete algorithms*, pages 1027–1035, 2007.
- [6] Colin Atkinson and Ann FS Mitchell. Rao’s distance measure. *Sankhyā: The Indian Journal of Statistics, Series A*, pages 345–365, 1981.

Table 2: k -center clustering accuracy in percentage on randomly generated datasets based on different geometries. The table shows the mean and standard deviation after 300 independent runs for each configuration. ρ is the distance measure. n is sample size of multinomial distributions. d is the dimension of the statistical simplex. σ is noise level.

ρ		ρ_{FHR}	ρ_{HG}	ρ_{IG}	$\rho_{\text{IG}} (k\text{-means})$	ρ_{EUC}	
3 clusters $n = 50$	$d = 9$	$\sigma = 0.5$	91.6 ± 14.3	94.0 ± 13.3	90.9 ± 14.3	93.8 ± 14.6	83.9 ± 15.8
		$\sigma = 0.9$	75.8 ± 14.1	84.9 ± 14.3	74.1 ± 14.1	81.0 ± 15.6	66.0 ± 12.4
		$\sigma = 1.3$	62.5 ± 11.1	71.8 ± 14.2	60.9 ± 10.3	65.2 ± 12.0	55.6 ± 9.6
	$d = 255$	$\sigma = 0.5$	95.1 ± 11.9	96.3 ± 11.1	94.8 ± 12.2	94.6 ± 13.8	92.3 ± 14.4
		$\sigma = 0.9$	86.3 ± 15.4	92.0 ± 13.8	84.0 ± 15.9	93.3 ± 14.7	68.8 ± 17.8
		$\sigma = 1.3$	79.0 ± 15.2	85.2 ± 15.9	74.7 ± 15.7	80.9 ± 17.9	45.3 ± 10.3
3 clusters $n = 100$	$d = 9$	$\sigma = 0.5$	92.8 ± 13.0	95.7 ± 11.5	92.4 ± 12.4	95.7 ± 12.8	84.1 ± 14.1
		$\sigma = 0.9$	75.9 ± 13.8	84.6 ± 14.7	74.1 ± 13.2	87.3 ± 12.6	64.4 ± 11.0
		$\sigma = 1.3$	61.8 ± 11.3	71.9 ± 13.6	60.4 ± 10.6	68.5 ± 12.9	54.7 ± 8.7
	$d = 255$	$\sigma = 0.5$	95.2 ± 12.5	96.8 ± 10.4	95.1 ± 11.9	94.5 ± 14.0	91.2 ± 15.6
		$\sigma = 0.9$	89.1 ± 14.6	92.1 ± 13.9	85.7 ± 15.6	93.4 ± 15.4	66.7 ± 18.1
		$\sigma = 1.3$	82.7 ± 14.8	88.4 ± 14.3	77.7 ± 15.6	90.0 ± 16.8	42.7 ± 9.3
5 clusters $n = 50$	$d = 9$	$\sigma = 0.5$	84.7 ± 12.7	88.8 ± 12.8	84.5 ± 12.4	87.9 ± 13.2	74.6 ± 11.7
		$\sigma = 0.9$	64.9 ± 10.6	75.0 ± 12.2	62.8 ± 10.5	68.0 ± 11.2	54.6 ± 8.3
		$\sigma = 1.3$	51.0 ± 7.8	61.1 ± 10.7	50.0 ± 7.5	51.9 ± 8.2	45.7 ± 6.3
	$d = 255$	$\sigma = 0.5$	92.5 ± 11.5	93.8 ± 11.0	92.6 ± 11.1	91.8 ± 12.3	87.3 ± 12.6
		$\sigma = 0.9$	81.4 ± 12.6	89.7 ± 12.3	78.2 ± 13.3	84.9 ± 14.5	64.1 ± 14.2
		$\sigma = 1.3$	71.9 ± 12.7	80.8 ± 13.2	69.6 ± 13.8	70.6 ± 14.4	36.7 ± 8.5
5 clusters $n = 100$	$d = 9$	$\sigma = 0.5$	85.1 ± 11.8	88.8 ± 12.8	83.6 ± 13.0	88.5 ± 13.3	74.5 ± 10.9
		$\sigma = 0.9$	62.8 ± 10.2	75.9 ± 12.3	61.1 ± 9.9	70.5 ± 11.2	52.0 ± 7.7
		$\sigma = 1.3$	49.0 ± 6.5	60.0 ± 11.3	47.8 ± 6.9	51.2 ± 8.1	43.5 ± 6.1
	$d = 255$	$\sigma = 0.5$	93.0 ± 11.3	93.2 ± 11.3	92.3 ± 11.3	91.4 ± 12.5	88.2 ± 12.4
		$\sigma = 0.9$	85.2 ± 11.9	89.1 ± 12.4	80.7 ± 12.5	87.8 ± 14.4	61.3 ± 14.2
		$\sigma = 1.3$	75.4 ± 12.3	82.0 ± 12.7	70.0 ± 13.2	79.1 ± 14.6	32.6 ± 7.8

- [7] Olivier Bachem, Mario Lucic, S. Hamed Hassani, and Andreas Krause. Approximate k-means++ in sublinear time. In *AAAI*, pages 1459–1467, 2016.
- [8] Olivier Bachem, Mario Lucic, and Andreas Krause. Scalable and distributed clustering via lightweight coresets. *arXiv preprint arXiv:1702.08248*, 2017.
- [9] Mihai Bădoiu and Kenneth L. Clarkson. Smaller core-sets for balls. In *ACM-SIAM Symposium on Discrete Algorithms*, pages 801–802, 2003.
- [10] Mihai Bădoiu and Kenneth L. Clarkson. Optimal core-sets for balls. *Computational Geometry*, 40(1):14–22, 2008.
- [11] Andreas Bernig. Hilbert geometry of polytopes. *Archiv der Mathematik*, 92(4):314–324, 2009.
- [12] Yanhong Bi, Bin Fan, and Fuchao Wu. Beyond Mahalanobis metric: Cayley-Klein metric learning. In *CVPR*, pages 2339–2347, 2015.
- [13] H. Busemann. *The Geometry of Geodesics*. Pure and Applied Mathematics. Elsevier Science, 2011.
- [14] Ovidiu Calin and Constantin Udriste. *Geometric Modeling in Probability and Statistics*. Mathematics and Statistics. Springer International Publishing, 2014.

- [15] N.N. Cencov. *Statistical Decision Rules and Optimal Inference*. Translations of mathematical monographs. American Mathematical Society, 2000.
- [16] Kamalika Chaudhuri and Andrew McGregor. Finding metric structure in information theoretic clustering. In *COLT*, pages 391–402, 2008.
- [17] Pierre de la Harpe. *On Hilbert’s metric for simplices*. 1991.
- [18] Michel Deza and Mathieu Dutour Sikirić. Voronoi polytopes for polyhedral norms on lattices. *Discrete Applied Mathematics*, 197:42–52, 2015.
- [19] J. G. Dowty. Chentsov’s theorem for exponential families. *ArXiv*, January 2017.
- [20] Yasunori Endo and Sadaaki Miyamoto. Spherical k -means++ clustering. In *Modeling Decisions for Artificial Intelligence*, pages 103–114. Springer, 2015.
- [21] Thomas Foertsch and Anders Karlsson. Hilbert metrics and Minkowski norms. *Journal of Geometry*, 83(1-2):22–31, 2005.
- [22] Teofilo F Gonzalez. Clustering to minimize the maximum intercluster distance. *Theoretical Computer Science*, 38:293–306, 1985.
- [23] David Hilbert. Über die gerade Linie als kürzeste Verbindung zweier Punkte. *Mathematische Annalen*, 46(1):91–96, 1895.
- [24] Harold Hotelling. Spaces of statistical parameters. In *Bulletin AMS*, volume 36, page 191, 1930.
- [25] Robert Jenssen, Jose C Principe, Deniz Erdogmus, and Torbjørn Eltoft. The Cauchy-Schwarz divergence and Parzen windowing: Connections to graph theory and mercer kernels. *Journal of the Franklin Institute*, 343(6):614–629, 2006.
- [26] Robert E. Kass and Paul W. Vos. *Geometrical Foundations of Asymptotic Inference*. Wiley-Interscience, 1997.
- [27] Mohammadali Khosravifard, Dariush Fooladivanda, and T Aaron Gulliver. Confliction of the convexity and metric properties in f -divergences. *IEICE Transactions on Fundamentals of Electronics, Communications and Computer Sciences*, 90(9):1848–1853, 2007.
- [28] M.C. Körner. *Minisum Hyperspheres*. Springer Optimization and Its Applications. Springer New York, 2011.
- [29] David H Laidlaw and Joachim Weickert. *Visualization and Processing of Tensor Fields: Advances and Perspectives*. Springer Science & Business Media, 2009.
- [30] Guy Lebanon. Learning Riemannian metrics. In *UAI*, pages 362–369, 2002.
- [31] Bas Lemmens and Roger Nussbaum. Birkhoff’s version of Hilbert’s metric and its applications in analysis. *Handbook of Hilbert Geometry*, pages 275–303, 2014.
- [32] Bas Lemmens and Cormac Walsh. Isometries of polyhedral hilbert geometries. *Journal of Topology and Analysis*, 3(02):213–241, 2011.
- [33] Xiao Liang. A note on divergences. *Neural Computation*, 28(10):2045–2062, 2016.
- [34] Bodo Manthey and Heiko Röglin. Worst-case and smoothed analysis of k -means clustering with Bregman divergences. *Journal of Computational Geometry*, 4(1):94–132, 2013.

- [35] Frank Nielsen and Gaëtan Hadjeres. Approximating covering and minimum enclosing balls in Hyperbolic geometry. In *International Conference on Networked Geometric Science of Information*, pages 586–594. Springer, 2015.
- [36] Frank Nielsen, Boris Muzellec, and Richard Nock. Classification with mixtures of curved Mahalanobis metrics. In *IEEE International Conference on Image Processing (ICIP)*, pages 241–245, 2016.
- [37] Frank Nielsen, Boris Muzellec, and Richard Nock. Large margin nearest neighbor classification using curved Mahalanobis distances. *CoRR*, abs/1609.07082, 2016.
- [38] Frank Nielsen and Richard Nock. On approximating the smallest enclosing Bregman balls. In *Proceedings of the 22nd annual symposium on Computational geometry (SoCG)*, pages 485–486. ACM, 2006.
- [39] Frank Nielsen and Richard Nock. On the smallest enclosing information disk. *Information Processing Letters*, 105(3):93–97, 2008.
- [40] Frank Nielsen and Richard Nock. Total Jensen divergences: Definition, properties and k-means++ clustering. *arXiv preprint arXiv:1309.7109*, 2013.
- [41] Frank Nielsen, Richard Nock, and Shun-ichi Amari. On clustering histograms with k -means by using mixed α -divergences. *Entropy*, 16(6):3273–3301, 2014.
- [42] Frank Nielsen and Laetitia Shao. On balls in a polygonal Hilbert geometry. In *33rd International Symposium on Computational Geometry (SoCG 2017)*, Dagstuhl, Germany, 2017. Schloss Dagstuhl–Leibniz-Zentrum fuer Informatik.
- [43] Frank Nielsen, Ke Sun, and Stéphane Marchand-Maillet. On Hölder projective divergences. *Entropy*, 19(3), 2017.
- [44] Richard Nock and Frank Nielsen. Fitting the smallest enclosing Bregman ball. In *ECML*, pages 649–656. Springer, 2005.
- [45] C Radhakrishna Rao. Information and accuracy attainable in the estimation of statistical parameters. *Bull. Cal. Math. Soc.*, 37(3):81–91, 1945.
- [46] C Radhakrishna Rao. Information and the accuracy attainable in the estimation of statistical parameters. In *Breakthroughs in statistics*, pages 235–247. Springer, 1992.
- [47] Daniel Reem. The geometric stability of Voronoi diagrams in normed spaces which are not uniformly convex. *CoRR*, abs/1212.1094, 2012.
- [48] Jürgen Richter-Gebert. *Perspectives on projective geometry: A guided tour through real and complex geometry*. Springer Science & Business Media, 2011.
- [49] Zhongmin Shen. Riemann-Finsler geometry with applications to information geometry. *Chinese Annals of Mathematics-Series B*, 27(1):73–94, 2006.
- [50] Hirohiko Shima. *The geometry of Hessian structures*. World Scientific, 2007.
- [51] Stephen M Stigler et al. The epic story of maximum likelihood. *Statistical Science*, 22(4):598–620, 2007.